AMERICAN SOCIETY FOR MICROBIOLOGY | Journal of Virology

Lipid Membranes Facilitate Conformational Changes Required for Reovirus Cell Entry

Anthony J. Snyder, Pranav Danthi

Department of Biology, Indiana University, Bloomington, Indiana, USA

ABSTRACT

Cellular entry of nonenveloped and enveloped viruses is often accompanied by dramatic conformational changes within viral structural proteins. These rearrangements are triggered by a variety of mechanisms, such as low pH, virus-receptor interactions, and virus-host chaperone interactions. Reoviruses, a model system for entry of nonenveloped viruses, undergo a series of disassembly steps within the host endosome. One of these steps, infectious subviral particle (ISVP)-to-ISVP* conversion, is necessary for delivering the genome-containing viral core into host cells, but the physiological trigger that mediates ISVP-to-ISVP* conversion during cell entry is unknown. Structural studies of the reovirus membrane penetration protein, μ1, predict that interactions between μ1 and negatively charged lipid head groups may promote ISVP* formation; however, experimental evidence for this idea is lacking. Here, we show that the presence of polyanions (SO_4^{2-} and HPO_4^{2-}) or lipids in the form of liposomes facilitates ISVP-to-ISVP* conversion. The requirement for charged lipids appears to be selective, since phosphatidylcholine and phosphatidylethanolamine promoted ISVP* formation, whereas other lipids, such as sphingomyelin and sulfatide, either did not affect ISVP* formation or prevented ISVP* formation. Thus, our work provides evidence that interactions with membranes can function as a trigger for a nonenveloped virus to gain entry into host cells.

IMPORTANCE

Cell entry, a critical stage in the virus life cycle, concludes with the delivery of the viral genetic material across host membranes. Regulated structural transitions within nonenveloped and enveloped viruses are necessary for accomplishing this step; these conformational changes are predominantly triggered by low pH and/or interactions with host proteins. In this work, we describe a previously unknown trigger, interactions with lipid membranes, which can induce the structural rearrangements required for cell entry. This mechanism operates during entry of mammalian orthoreoviruses. We show that interactions between reovirus entry intermediates and lipid membranes devoid of host proteins promote conformational changes within the viral outer capsid that lead to membrane penetration. Thus, this work illustrates a novel strategy that nonenveloped viruses can use to gain access into cells and how viruses usurp disparate host factors to initiate infection.

Nonenveloped and enveloped viruses undergo significant structural rearrangements that facilitate their entry into host cells. These conformational changes, which are required for delivering the viral genetic material across cellular membranes, can be triggered by one or more mechanisms. Low pH promotes genome release during rhinovirus infection (1, 2) and fusion between viral and host membranes during influenza virus infection (3–5). Virus-receptor interactions induce viral uncoating during poliovirus infection (6–8) and membrane fusion during herpesvirus infection (9–11). Avian retroviruses (enveloped) use both receptor binding and low pH to promote membrane fusion (12). Host chaperones activate polyomaviruses, which enables virus translocation across the endoplasmic reticulum membrane (13–15). Thus, low pH and protein-protein interactions are thought to be the predominant triggers that facilitate viral entry.

Mammalian orthoreoviruses (reoviruses) serve as versatile experimental models for studies of virus entry. Reoviruses are nonenveloped, double-stranded RNA viruses that are composed of two concentric protein shells: the inner capsid (core) and the outer capsid (16, 17). To initiate infection, the outer capsid must undergo a series of disassembly events that conclude with core release into the host cytoplasm. Following attachment to protein or carbohydrate receptors (18–22), virions are endocytosed (23–28) and the σ3 protector protein is degraded by endosomal cathepsin proteases (24, 28–33). This process generates a metastable intermediate, called infectious subviral particles (ISVPs), in which the cell penetration protein, μ1, is exposed (16). Within the intestinal tract, ISVPs are generated extracellularly by luminal proteases, such as chymotrypsin (34–37). *In vitro*, ISVPs are produced by digesting purified virions with chymotrypsin (38, 39). In a manner analogous to that for the other viruses described above, reovirus ISVPs must undergo conformational changes to deposit the genome-containing core particle into the host cytoplasm. The conformationally altered particle is referred to as ISVP*. ISVP-to-ISVP* conversion results in cleavage and the release of μ1-derived pore-forming peptides (40–47). The released peptides form 4- to 10-nm pores within endosomal membranes, which are thought to mediate core delivery into the cytoplasm (40, 41, 48). While ISVP* formation can be triggered *in vitro* using heat, bovine red blood

Received 25 November 2015 **Accepted** 15 December 2015

Accepted manuscript posted online 23 December 2015

Citation Snyder AJ, Danthi P. 2016. Lipid membranes facilitate conformational changes required for reovirus cell entry. J Virol 90:2628–2638. doi:10.1128/JVI.02997-15.

Editor: S. López

Address correspondence to Pranav Danthi, pdanthi@indiana.edu.

Copyright © 2016, American Society for Microbiology. All Rights Reserved.

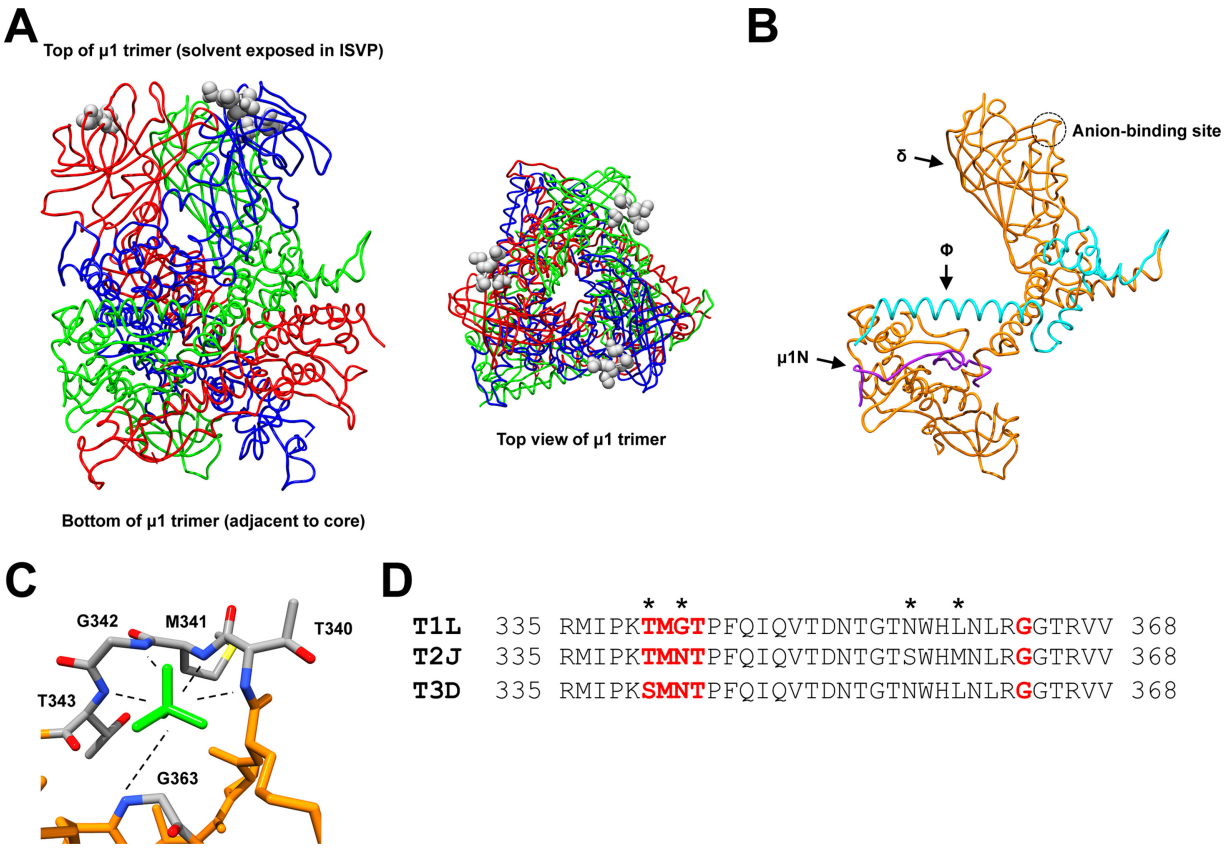

FIG 1 Structure and sequence of the reovirus μ1 protein. (A) Side and top views (left and right, respectively) of the T1L μ1 homotrimer (52) (PDB accession number 1JMU). Individual μ1 monomers are colored in red, blue, and green. Residues corresponding to the anion-binding site are represented as gray spheres. (B) Structure of the T1L μ1 monomer (52) (PDB accession number 1JMU). Purple, μ1N; teal, Φ; orange, δ. The anion-binding site is indicated with a circle. (C) Structure of the T1L μ1 anion-binding site (52) (PDB accession number 1JMU). Residues that form the anion-binding site are labeled and colored in gray (carbon), blue (nitrogen), red (oxygen), and yellow (sulfur). The sulfate ion is colored in green. (D) Amino acid sequence alignments of the reovirus μ1 anion-binding site. Residues that correspond to the anion-binding site are bolded in red. Residues that are not conserved within the sequence region are indicated with an asterisk.T1L, reovirus type 1 Lang; T2J, reovirus type 2 Jones; T3D, reovirus type 3 Dearing.

cells (RBCs), or large monovalent cations, such as Cs^+ or K^+ (42, 49–51), the physiological signal that facilitates ISVP* conversion is unknown.

The crystal structure of the native reovirus type 1 Lang (T1L) μ1 trimer revealed a polyanion (SO_4^{2-}) that binds in a well-ordered pocket at the tip of each μ1 monomer (which is solvent exposed in ISVPs) (Fig. 1A) (52). This pocket was called the anion-binding site and resembles loops that bind phosphates in nucleotide-binding proteins and protein kinases (Fig. 1C) (53, 54). Interestingly, the anion-binding site is located in the central, δ-fragment region of μ1 (Fig. 1B) (52). The δ fragment adopts a conformationally altered state during ISVP-to-ISVP* conversion (42). Thus, it was proposed that interactions between negatively charged lipids and the μ1 anion-binding site may function as an in-cell trigger for ISVP* formation (52).

In this work, we utilized a biochemical approach to investigate the role of host membranes during entry of two prototype reovirus strains. We show that polyanions (SO_4^{2-} and HPO_4^{2-}) promote ISVP* formation and enhance ISVP-induced hemolysis of RBCs. Using liposomes, we demonstrate that cellular proteins are not required for reoviruses to undergo ISVP-to-ISVP* conversion. We also present data indicating that while some lipids (phosphatidylcholine [PC] and phosphatidylethanolamine [PE]) promote ISVP-to-ISVP* conversion, others, such as cholesterol (Chl), sphingomyelin (SM), and lysobisphosphatidic acid (LBPA), have no impact on ISVP-to-ISVP* conversion. Together, the data obtained in this work provide evidence that interactions with lipid membranes can trigger the conformational changes required for cell entry of viruses.

MATERIALS AND METHODS

Cells and viruses. Murine L929 (L) cells were grown at 37°C in Joklik's minimal essential medium (Lonza, Walkersville, MD) supplemented with 5% fetal bovine serum (FBS; Life Technologies, Carlsbad, CA), 2 mM L-glutamine (Invitrogen, Carlsbad, CA), 100 U/ml penicillin (Invitrogen, Carlsbad, CA), 100 μg/ml streptomycin (Invitrogen, Carlsbad, CA), and 25 ng/ml amphotericin B (Sigma-Aldrich, St. Louis, MO). Reovirus type 3 Dearing (T3D) and T1L were generated by plasmid-based reverse genetics (55, 56).

Virus purification. T3D and T1L virions were propagated and purified as previously described (51, 57). Briefly, L cells infected with second- or third-passage reovirus stocks were lysed by sonication. Viral particles were extracted from lysates using Vertrel-XF specialty fluid (Dupont, Wilmington, DE) (58). The extracted particles were layered onto 1.2- to 1.4-g/cm^3 CsCl step gradients. The gradients were then centrifuged at 187,000 × *g* for 4 h at 4°C. Bands corresponding to purified virus particles (~1.36 g/cm^3) (59) were isolated and dialyzed into virus storage buffer

(10 mM Tris, pH 7.4, 15 mM $MgCl_2$, 150 mM NaCl). Following dialysis, the particle concentration was determined by measuring optical density of the purified virus stocks at 260 nm (OD_{260}; 1 unit at $OD_{260} = 2.1 \times 10^{12}$ particles/ml) (59).

Generation of ISVPs. T3D or T1L virions (2×10^{12} particles/ml) were digested with 200 μg/ml TLCK (*N*α-*p*-tosyl-L-lysine chloromethyl ketone)-treated chymotrypsin (Worthington Biochemical, Lakewood, NJ) in a total volume of 100 μl for 1 h at 32°C (38, 39). After 1 h, the reaction mixtures were incubated on ice for 20 min and quenched by the addition of 1 mM phenylmethylsulfonyl fluoride (Sigma-Aldrich, St. Louis, MO). The generation of ISVPs was confirmed by SDS-PAGE and Coomassie staining.

ISVP-to-ISVP* conversion assay. T3D or T1L ISVPs (2×10^{12} particles/ml) were incubated in the absence or presence of 300 mM CsCl, 180 mM $MgSO_4$, or 180 mM Na_2HPO_4 (see Fig. 3); 1 mM early endosome (EE) or late endosome (LE) liposomes (see Fig. 5); 1 mM early endosome, early endosome without phosphatidylethanolamine, early endosome without sphingomyelin, phosphatidylcholine, phosphatidylcholine-phosphatidylethanolamine (2:1), or phosphatidylcholine-sphingomyelin (5:1) liposomes (see Fig. 6); or 1 mM phosphatidylcholine, phosphatidylcholine-phosphatidic acid (PA) (5:1), or phosphatidylcholine-sulfatide (7:1) liposomes (see Fig. 7) for 1 h at the temperatures indicated below. After 1 h, the reaction mixtures were treated with 0.08 mg/ml trypsin (Sigma-Aldrich, St. Louis, MO) for 30 min on ice. Following digestion, the reaction mixtures were solubilized in reducing SDS sample buffer and analyzed by SDS-PAGE. The gels were Coomassie stained and imaged on an Odyssey imaging system (LI-COR, Lincoln, NE).

ISVP-induced hemolysis assay. Citrated bovine RBCs (Colorado Serum Company, Denver, CO) were pelleted for 5 min by centrifugation at 500 × *g* and resuspended in ice-cold phosphate-buffered saline (PBS) supplemented with 2 mM $MgCl_2$ (PBS^{Mg}). This step was repeated until the supernatant remained clear after pelleting. After washing, the RBCs were resuspended in PBS^{Mg} at a 30% (vol/vol) concentration. Hemolysis efficiency was determined by incubating a suboptimal number of T3D or T1L ISVPs (2×10^{12} particles/ml) in a 3% (vol/vol) solution of untreated RBCs (see above) or protease-treated RBCs ($RBCs^{PT}$; see "Generation of $RBCs^{PT}$" below). When indicated, the ISVP-RBC mixtures were supplemented with 300 mM CsCl, 180 $MgSO_4$, 180 $MgCl_2$, 180 mM NaH_2PO_4, or 180 mM Na_2HPO_4. Levels of 0 and 100% hemolysis were determined by incubating an equivalent number of RBCs in virus storage buffer (10 mM Tris, pH 7.4, 15 mM $MgCl_2$, 150 mM NaCl) or virus storage buffer supplemented with 0.8% Triton X-100, respectively. The samples were incubated for 2 h at 37°C. After 2 h, the reaction mixtures were placed on ice for 20 min, followed by centrifugation for 5 min at 500 × *g*. To quantify the amount of hemoglobin release, the supernatants were diluted 1:5 into virus storage buffer, and the absorbance at 405 nm (A_{405}) was measured using a microplate reader (Molecular Devices, Sunnyvale, CA). Percent hemolysis was calculated using the following formula: $[(A_{sample} - A_{buffer})/(A_{TX\text{-}100} - A_{buffer})] \times 100$, where A_{sample} is the absorbance of the sample, A_{buffer} is the absorbance of the buffer, and $A_{TX\text{-}100}$ is the absorbance of the buffer supplemented with 0.8% Triton X-100. *P* values were calculated using Student's *t* test.

Generation of $RBCs^{PT}$. $RBCs^{PT}$ were generated as previously described, with some exceptions (48). Briefly, citrated bovine RBCs (Colorado Serum Company, Denver, CO) were pelleted by centrifugation for 5 min at 500 × *g* and resuspended in ice-cold PBS^{Mg}. This step was repeated until the supernatant remained clear after pelleting. After washing, the RBCs were resuspended in PBS^{Mg} at a 10% (vol/vol) concentration. To treat the RBCs with protease, the resuspended RBCs were incubated with 0.25 mg/ml proteinase K (Sigma, St. Louis, MO) for 20 min at 37°C. After 20 min, the reaction was quenched with 2 mM phenylmethylsulfonyl fluoride (Sigma-Aldrich, St. Louis, MO) and the reaction mixture was incubated on ice for 15 min. The $RBCs^{PT}$ were then pelleted by centrifugation for 5 min at 500 × *g* and washed five times with PBS^{Mg}. After washing, the $RBCs^{PT}$ were resuspended in PBS^{Mg} at a 10% (vol/vol) concentration supplemented with 2 mM phenylmethylsulfonyl fluoride (Sigma, St. Louis, MO), and the mixture was incubated on ice for 15 min. Finally, the $RBCs^{PT}$ were pelleted by centrifugation for 5 min at 500 × *g* and washed five times with PBS^{Mg}. For use in hemolysis assays, the pelleted $RBCs^{PT}$ were resuspended in PBS^{Mg} at a 30% (vol/vol) concentration.

Liposome preparation. The lipids used in this study (L-α-phosphatidylcholine [PC] from chicken egg, L-α-phosphatidic acid [PA] from chicken egg, sulfatide from porcine brain, sphingomyelin [SM] from porcine brain, cholesterol [Chl] from ovine wool, L-α-phosphatidylethanolamine [PE] from chicken egg, L-α-phosphatidylserine [PS] from porcine brain, and lysobisphosphatidic acid [LBPA]) were purchased from Avanti Polar Lipids (Alabaster, AL). All lipids were dissolved in chloroform and stored at −20°C, except for sulfatide, which was dissolved in chloroform-methanol-water (2:1:0.1). Prior to liposome preparation, the lipids were dried under a stream of argon gas. Liposomes were prepared by resuspending the dried lipids in 250 μl of virus storage buffer (10 mM Tris, pH 7.4, 15 mM $MgCl_2$, 150 mM NaCl) and passing the resuspension (31 times) through an Avanti miniextruder with a 0.1-μm-pore-size (for ISVP-to-ISVP* conversion assay) or 0.4-μm-pore-size [for 5(6)-carboxyfluorescein (CF)-loaded liposome pore formation assay] polycarbonate membrane (Avanti Polar Lipids, Alabaster, AL). The liposome compositions used in this study were PC, PC-PE (2:1 molar ratio), PC-SM (5:1 molar ratio), PC-PA (5:1 molar ratio), and PC-sulfatide (7:1 molar ratio). The compositions of early and late endosome liposomes are shown in Fig. 5A (60).

Generation of CF-loaded liposomes. CF-loaded liposomes were generated as previously described, with some exceptions (48). Briefly, CF was purchased from Acros Organics (Geel, Belgium). CF-loaded liposomes were prepared following the liposome preparation method described above, with the exception that dried lipids were resuspended in 250 μl of CF solution (22 mg/ml). CF solution was prepared by mixing CF in virus storage buffer (10 mM Tris, pH 7.4, 15 mM $MgCl_2$, 150 mM NaCl) and adding drops of 10 M NaOH until the mixture became clear. Following extrusion, CF-loaded liposomes were separated from unincorporated dye using 10DG desalting columns (Bio-Rad, Hercules, CA) that had been equilibrated with virus storage buffer following the manufacturer's protocol. Fractions of 0.5 ml were collected by elution with virus storage buffer. Fractions containing CF-loaded liposomes were identified by diluting 1 μl of each fraction into 99 μl of virus storage buffer or virus storage buffer supplemented with 0.5% Triton X-100 and measuring the fluorescence (excitation at 485 nm, emission at 528 nm) using a Synergy H1 hybrid plate reader (BioTek, Winooski, VT).

ISVP, CF-loaded liposome pore formation assay. T3D or T1L ISVPs (2×10^{12} particles/ml) were incubated with 10 μl of CF-loaded PC, PC-sulfatide (7:1), PC-PE (2:1), early endosome, or early endosome without PE liposomes (final reaction volume, 20 μl) for 1 h at the temperatures indicated below. After 1 h, the reaction mixtures were diluted 1:50 into virus storage buffer (10 mM Tris, pH 7.4, 15 mM $MgCl_2$, 150 mM NaCl). The samples were allowed to equilibrate at room temperature for 15 min, and the fluorescence (excitation at 485 nm, emission at 528 nm) was measured using a Synergy H1 hybrid plate reader (BioTek, Winooski, VT). The percent CF leakage was calculated using the following formula: $[(A_{sample} - A_{buffer})/(A_{TX\text{-}100} - A_{buffer})] \times 100$. *P* values were calculated using Student's *t* test.

RESULTS

SO_4^{2-} and HPO_4^{2-} polyanions promote ISVP-induced hemolysis and ISVP-to-ISVP* conversion. The crystal structure of the T1L μ1 homotrimer revealed an anion-binding site at the tip of each μ1 monomer. These sites coordinated sulfate ions (Fig. 1). It was proposed that interactions between negatively charged lipid head groups and the anion-binding sites may promote ISVP* formation (52). Therefore, we sought to determine if polyanions in-

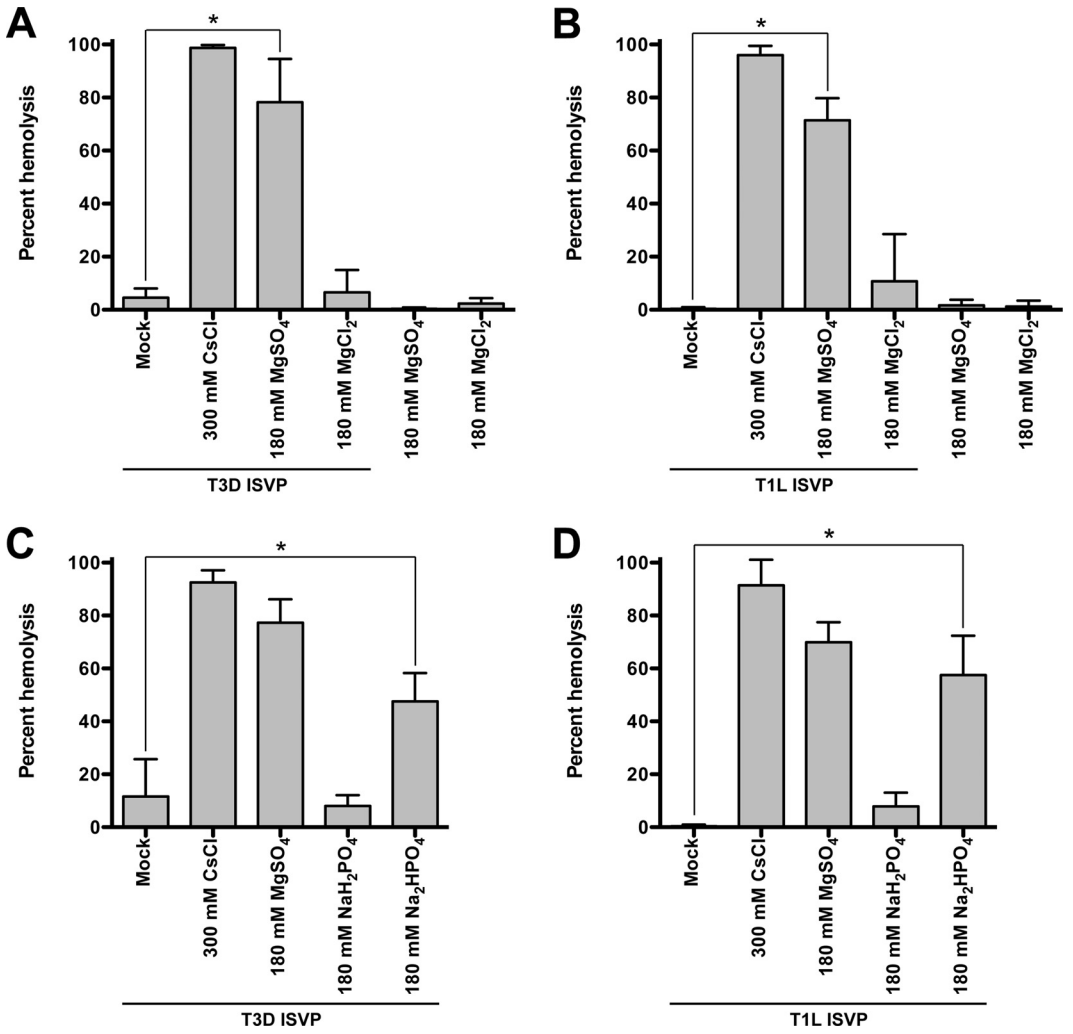

FIG 2 SO_4^{2-} and HPO_4^{2-} polyanions promote ISVP-induced hemolysis. T3D (A and C) or T1L (B and D) ISVPs (2×10^{12} particles/ml) were incubated in a 3% (vol/vol) solution of untreated bovine red blood cells supplemented with 300 mM CsCl, 180 mM $MgSO_4$, or 180 mM $MgCl_2$ (A and B) or 300 mM CsCl, 180 mM $MgSO_4$, 180 mM NaH_2PO_4, or 180 mM Na_2HPO_4 (C and D) for 2 h at 37°C. After 2 h, hemolysis was quantified by measuring the absorbance of the supernatant at 405 nm. Levels of 0 and 100% hemolysis were determined by incubating an equivalent number of RBCs in virus storage buffer or virus storage buffer supplemented with 0.8% Triton X-100, respectively, for 2 h at 37°C. For each condition, the mean percent hemolysis was determined from at least three independent experiments. Error bars indicate standard deviations. *P* values were calculated using Student's *t* test. *, $P \leq 0.05$.

fluence ISVP-to-ISVP* conversion for two prototype reovirus strains, type 3 Dearing (T3D) and type 1 Lang (T1L).

ISVP* formation and perforation of the endosomal membrane can be recapitulated *in vitro* by examining the capacity of ISVPs to induce hemolysis of bovine red blood cells (RBCs) (42, 51). The extent of RBC hemolysis and, thus, ISVP-to-ISVP* conversion is measured by determination of the amount of hemoglobin released into the supernatant. To test if anions can facilitate ISVP* formation and hemolysis, T3D or T1L ISVPs were incubated with untreated RBCs in the absence or presence of $MgSO_4$ or $MgCl_2$ (Fig. 2A and B) or NaH_2PO_4 or Na_2HPO_4 (Fig. 2C and D) for 2 h at 37°C. For comparison, we incubated ISVPs with untreated RBCs in the presence of CsCl, which is a known trigger for ISVP-to-ISVP* conversion (42, 49). Compared to the level of hemolysis achieved with ISVPs alone, we observed a significant increase in the level of hemolysis when T3D or T1L ISVPs were incubated with $MgSO_4$ or Na_2HPO_4 but not when RBCs were incubated with $MgCl_2$ or NaH_2PO_4.

Concurrently with ISVP-to-ISVP* conversion, the reovirus outer capsid protein, μ1, undergoes a conformational change that renders μ1 susceptible to proteolysis (42). This structural rearrangement is assayed *in vitro* by heating ISVPs and determining the susceptibility of the δ fragment (a product of μ1 cleavage during ISVP formation) to trypsin digestion (42, 50). To further test if polyanions can promote ISVP* formation, we compared the efficiency of heat-induced ISVP-to-ISVP* conversion in the absence and presence of $MgSO_4$ or Na_2HPO_4 (Fig. 3). Compared to ISVPs alone, inclusion of SO_4^{2-} or HPO_4^{2-} reduced the temperature required to render the δ fragment trypsin sensitive. T3D and T1L ISVPs alone converted to ISVP*s at 42°C and 43°C, respectively (Fig. 3B and data not shown), whereas SO_4^{2-} reduced the transition temperature to 39°C (T3D) and 41°C (T1L). HPO_4^{2-} reduced the transition temperatures to 40°C (T3D) and 41°C (T1L). Together, these findings support the hypothesis that interactions between ISVPs and polyanions, namely, SO_4^{2-} and HPO_4^{2-}, can enhance ISVP* formation.

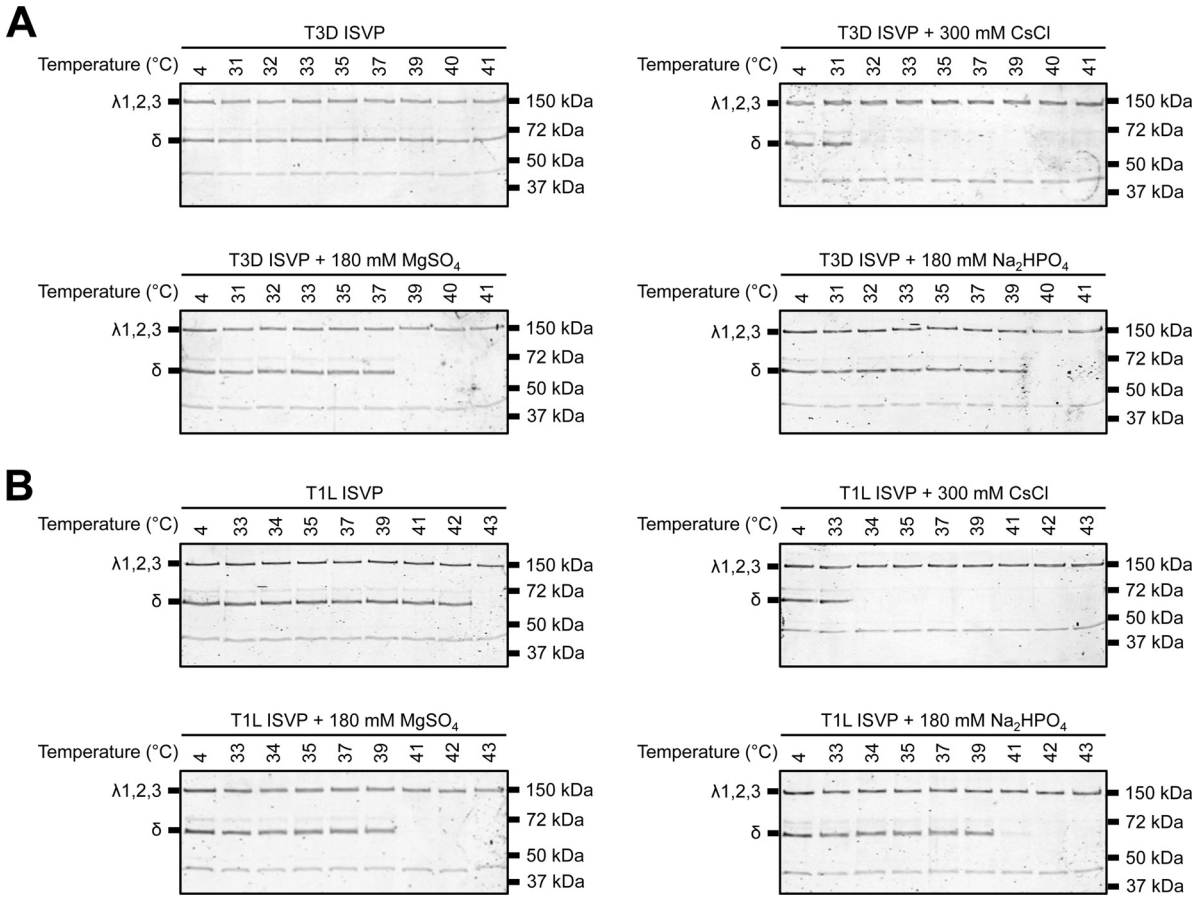

FIG 3 SO_4^{2-} and HPO_4^{2-} polyanions promote ISVP-to-ISVP* conversion. T3D (A) or T1L (B) ISVPs (2×10^{12} particles/ml) were incubated in virus storage buffer supplemented with 300 mM CsCl, 180 mM $MgSO_4$, or 180 mM Na_2HPO_4 for 1 h at the indicated temperatures. After 1 h, the reaction mixtures were treated with trypsin (0.08 mg/ml) for 30 min on ice. Following digestion, the reaction mixtures were solubilized in reducing SDS sample buffer and analyzed by SDS-PAGE. The gels were Coomassie stained. The migration of the λ1,2,3 and δ bands is indicated to the left of each panel. The migration of molecular mass markers is indicated to the right of each panel.

Proteolysis of cell surface proteins renders RBCs more susceptible to ISVP-induced hemolysis. During cell entry, ISVPs are unlikely to encounter polyanions at the concentration used in the assays whose results are presented in Fig. 2 and 3. Therefore, we considered the hypothesis that negatively charged proteins or lipids present on the host membrane may trigger ISVP-to-ISVP* conversion. To test this idea, we compared the capacity of ISVPs to induce the hemolysis of untreated (control) or protease-treated RBCs. Proteinase K treatment of RBCs, which is expected to remove the majority of extracellular domains from membrane proteins (48), resulted in enhanced T3D or T1L ISVP-induced hemolysis (Fig. 4A and B, respectively). These data suggest that interactions between ISVPs and lipid membranes, rather than interactions between ISVPs and membrane proteins, mediate ISVP* formation and hemolysis. Furthermore, the enhancement of hemolysis following protease treatment suggests that RBC surface proteins may hinder ISVP-to-ISVP* conversion by limiting the access of ISVPs to the lipid components of host membranes.

Liposomes promote ISVP-to-ISVP* conversion in a lipid composition-dependent manner. Thus far, our results suggest a role for lipids, specifically, negatively charged head groups, in facilitating ISVP-to-ISVP* conversion. To directly test this idea, we generated liposomes that resemble the lipid compositions of early endosomal or late endosomal membranes (referred to as EE and LE liposomes, respectively) (Fig. 5A) (60) and tested their capacity to induce ISVP-to-ISVP* conversion. The acquisition of a trypsin-sensitive conformation of the μ1 δ fragment was assayed as a readout for ISVP* formation (Fig. 5B). T3D ISVPs alone did not undergo the conformational changes required to render δ protease sensitive at temperatures up to 41°C. In contrast, T3D ISVPs incubated in the presence of EE or LE liposomes underwent ISVP-to-ISVP* conversion at 37°C. These data support the idea that lipids devoid of host proteins can trigger the conformational changes required for reovirus cell entry.

We next sought to determine if the specific lipids that make up the endosomal membrane differentially impact ISVP-to-ISVP* conversion. Because EE and LE liposomes promote ISVP* formation to an equivalent extent, we reasoned that a component common to these compartments would likely have the most significant impact on lowering the temperature needed to trigger ISVP* formation. To test this idea, we excluded one lipid at a time from EE liposomes (Fig. 6A). We found that removing PE from the EE liposomes rendered ISVP* formation less efficient. In contrast, removing SM from EE liposomes enhanced ISVP* formation. Removing cholesterol, PS, or LBPA had no impact on ISVP-to-ISVP* conversion (data not shown). Since PC is a major compo-

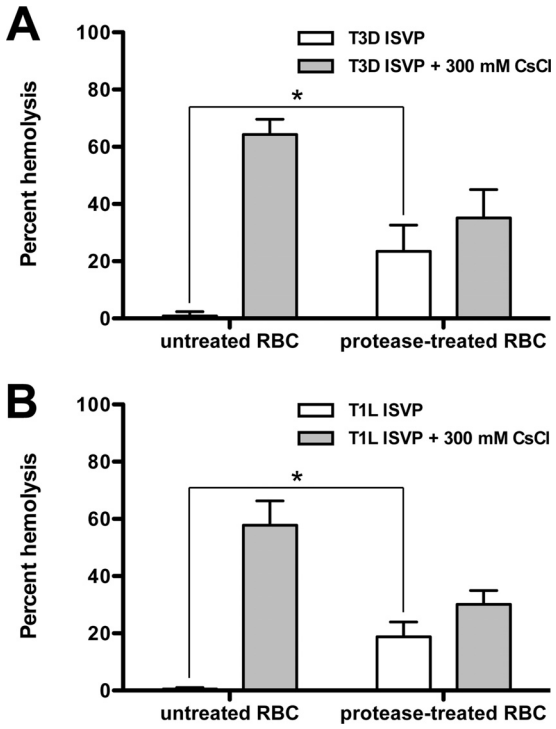

FIG 4 ISVP-induced hemolysis of untreated and protease-treated RBCs. T3D (A) or T1L (B) ISVPs (2×10^{12} particles/ml) were incubated in a 3% (vol/vol) solution of untreated or protease-treated bovine RBCs in the absence or presence of 300 mM CsCl for 2 h at 37°C. After 2 h, hemolysis was quantified by measuring the absorbance of the supernatant at 405 nm. Levels of 0 and 100% hemolysis were determined by incubating an equivalent number of RBCs in virus storage buffer or virus storage buffer supplemented with 0.8% Triton X-100, respectively, for 2 h at 37°C. For each condition, the mean percent hemolysis was determined from at least three independent experiments. Error bars indicate standard deviations. *P* values were calculated using Student's *t* test. *, $P \leq 0.05$.

A

Lipid	Early endosome (EE) liposomes[a]	Late endosome (LE) liposomes[a]
Chl	50	34
PC	26	37
PE	13	14
SM	5	2
PS	5	3
LBPA	1	10

[a] Values indicate mol% of lipids in EE or LE liposomes

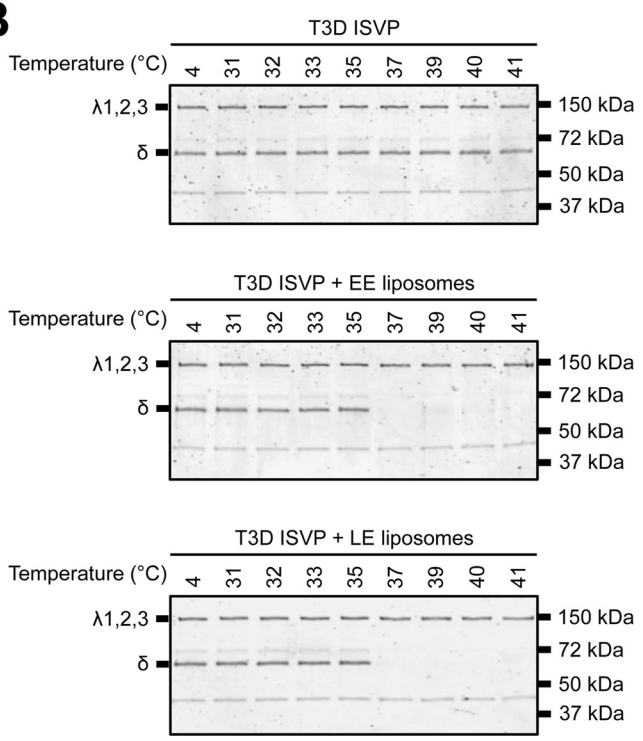

FIG 5 Liposomes that mimic the composition of the early or late endosomal membranes facilitate ISVP-to-ISVP* conversion. (A) Lipid compositions of the EE and LE liposomes. (B) EE or LE liposome-mediated ISVP-to-ISVP* conversion. T3D ISVPs (2×10^{12} particles/ml) were incubated in virus storage buffer supplemented with 1 mM EE or LE liposomes for 1 h at the indicated temperatures. After 1 h, the reaction mixtures were treated with trypsin (0.08 mg/ml) for 30 min on ice. Following digestion, the reaction mixtures were solubilized in reducing SDS sample buffer and analyzed by SDS-PAGE. The gels were Coomassie stained. The migration of the λ1,2,3 and δ bands is indicated to the left of each panel. The migration of molecular mass markers is indicated to the right of each panel.

nent of EE liposomes, we also tested the capacity of PC-only liposomes to facilitate ISVP-to-ISVP* conversion (Fig. 6B). PC liposomes reduced the temperature required to trigger ISVP* formation to 39°C. Furthermore, liposomes containing PC and PE induced ISVP* formation at the same temperature as EE liposomes (compare Fig. 6A and B). In contrast, liposomes containing PC and SM promoted ISVP* formation with the same efficiency as PC-only liposomes (Fig. 6B). Together, these data indicate that ISVP-to-ISVP* conversion can be induced by specific lipids (i.e., PC and PE).

Our original hypothesis was that negatively charged lipid head groups interact with the μ1 anion-binding site to promote the conformational changes required for reovirus cell entry. To gain a better understanding of lipid-mediated ISVP-to-ISVP* conversion, we generated PC liposomes that contain phosphatidic acid (PA) or sulfatide. Neither of these lipids is a main constituent of the plasma or endosomal membranes (60), but each contains a negatively charged head group. Among these, sulfatide is particularly interesting because this lipid is present within the extracellular leaflet of RBC membranes (61). Compared to PC liposomes, inclusion of PA did not significantly change the temperature at which ISVP-to-ISVP* conversion occurred (Fig. 7). In contrast, inclusion of sulfatide prevented PC-induced ISVP* formation; the δ fragment remained protease sensitive at temperatures up to 41°C. Although these data do not help us understand the basis for why some lipids but not others promote ISVP-to-ISVP* conversion, these results further indicate that liposome-mediated ISVP* formation occurs in a lipid composition-dependent manner.

The results presented here demonstrate that lipids can trigger ISVP-to-ISVP* conversion. Nonetheless, PC and PE (which contain neutral, zwitterionic head groups) enhance ISVP* formation (Fig. 6), whereas PS (which contains a negatively charged head group) does not (data not shown). Furthermore, PA and sulfatide either minimally impacted or negatively impacted the efficiency of ISVP-to-ISVP* conversion (Fig. 7). These results indicate that fac-

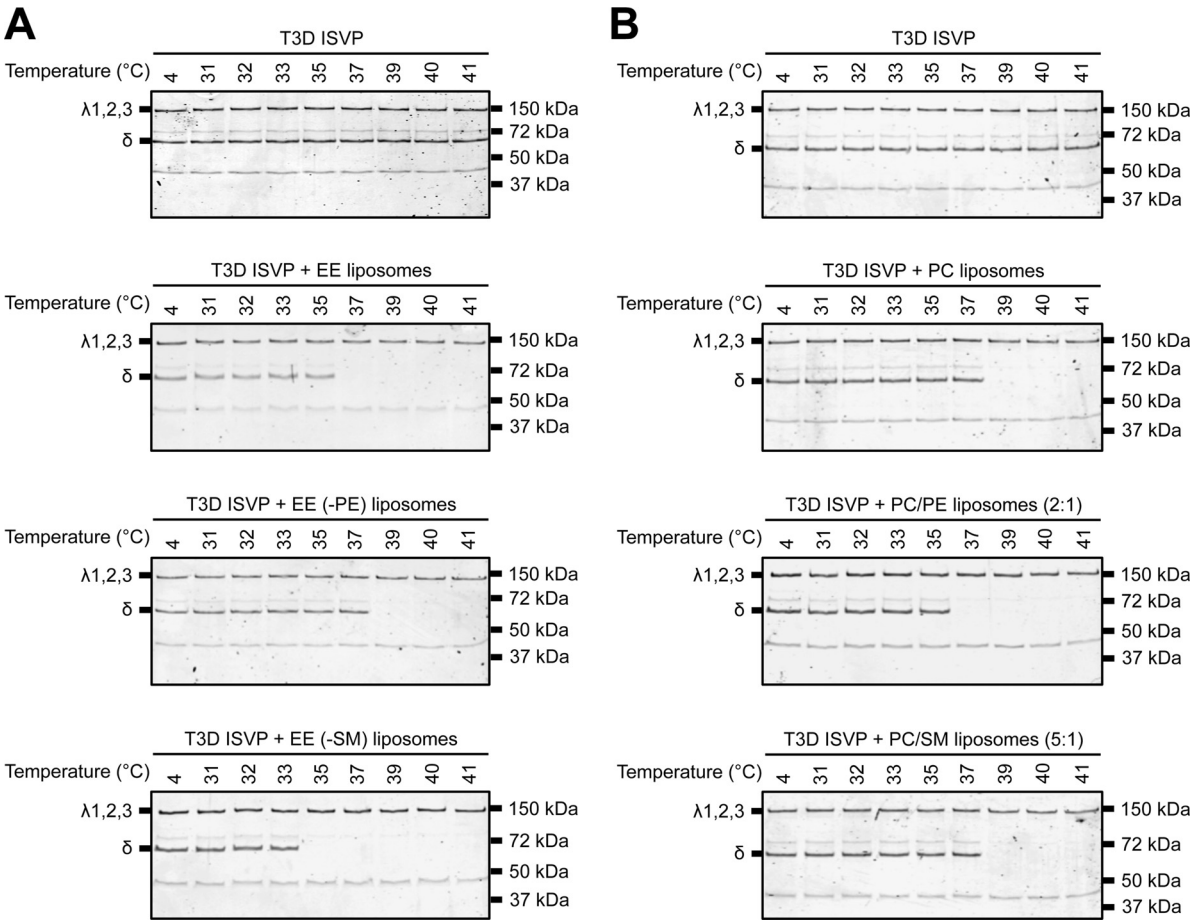

FIG 6 PC and PE are the main contributors to lipid-mediated ISVP-to-ISVP* conversion. T3D ISVPs (2×10^{12} particles/ml) were incubated in virus storage buffer supplemented with 1 mM EE, EE without PE, or EE without SM liposomes (A) or 1 mM PC, PC-PE (2:1), or PC-SM (5:1) liposomes for 1 h at the indicated temperatures. After 1 h, the reaction mixtures were treated with trypsin (0.08 mg/ml) for 30 min on ice. Following digestion, the reaction mixtures were solubilized in reducing SDS sample buffer and analyzed by SDS-PAGE. The gels were Coomassie stained. The migration of the λ1,2,3 and δ bands is indicated to the left of each panel. The migration of molecular mass markers is indicated to the right of each panel.

tors other than lipid head group composition may influence the efficiency of ISVP* formation.

Liposome-mediated ISVP-to-ISVP* conversion induces membrane penetration. As a consequence of ISVP* formation, reovirus particles release μ1 N- and C-terminal fragments, μ1N and Φ, respectively (40, 41, 47). These peptides form 4- to 10-nm pores in endosomal membranes, which are thought to mediate core delivery to the host cytoplasm (40, 41, 48). To assay pore formation, we generated carboxyfluorescein (CF)-loaded liposomes. The extent of CF release and, thus, ISVP* and pore formation was determined by measuring the fluorescence of dequenched CF (48). We incubated T3D ISVPs with CF-loaded EE liposomes or EE liposomes lacking PE for 1 h at 4°C, 30°C, or 42°C (Fig. 8A). Similarly, we incubated T3D ISVPs with CF-loaded PC or PC-PE (2:1) liposomes. As expected, we observed minimal (less than 5%) CF release when ISVPs were incubated with liposomes at 4°C (Fig. 8A and B, white bars). When ISVP-to-ISVP* conversion was triggered with heat (42°C), CF was released from each type of liposome at approximately equal levels (75 to 80%), demonstrating that pore formation can occur independently of the lipid compositions used in this work (Fig. 8A and B, black bars). We observed equivalent CF release after incubating ISVPs with each type of liposome at 30°C (Fig. 8A and B, gray bars). Thus, the CF release assay (where only a few μ1 monomers may need to undergo conformational changes to cause CF leakage) indicated that liposome-mediated ISVP* formation occurs at temperatures as low as 30°C. In contrast, the protease sensitivity assay (where nearly all μ1 δ fragments need to become protease sensitive to observe ISVP-to-ISVP* conversion) indicated that liposome-mediated ISVP* formation occurs at 35°C or higher.

Although the more sensitive CF release assay did not reveal lipid-specific effects on ISVP-to-ISVP* conversion, our data indicate that lipids drive ISVP* formation in a manner that is reminiscent of cell entry (i.e., the ability to generate pores). Using PC and PC-sulfatide (7:1) liposomes, which differ more dramatically in the capacity to induce ISVP-to-ISVP* conversion (Fig. 7), we observed a significant difference in ISVP-induced pore formation; CF was released from PC liposomes to a greater extent than PC-sulfatide (7:1) liposomes at 30°C (Fig. 8C; compare the gray bars). These data further indicate that specific lipids can trigger ISVP-to-ISVP* conversion and pore formation more efficiently than others.

T3D ISVPs induce pore formation more efficiently than T1L ISVPs. T1L and T3D are two natural reovirus isolates that are used

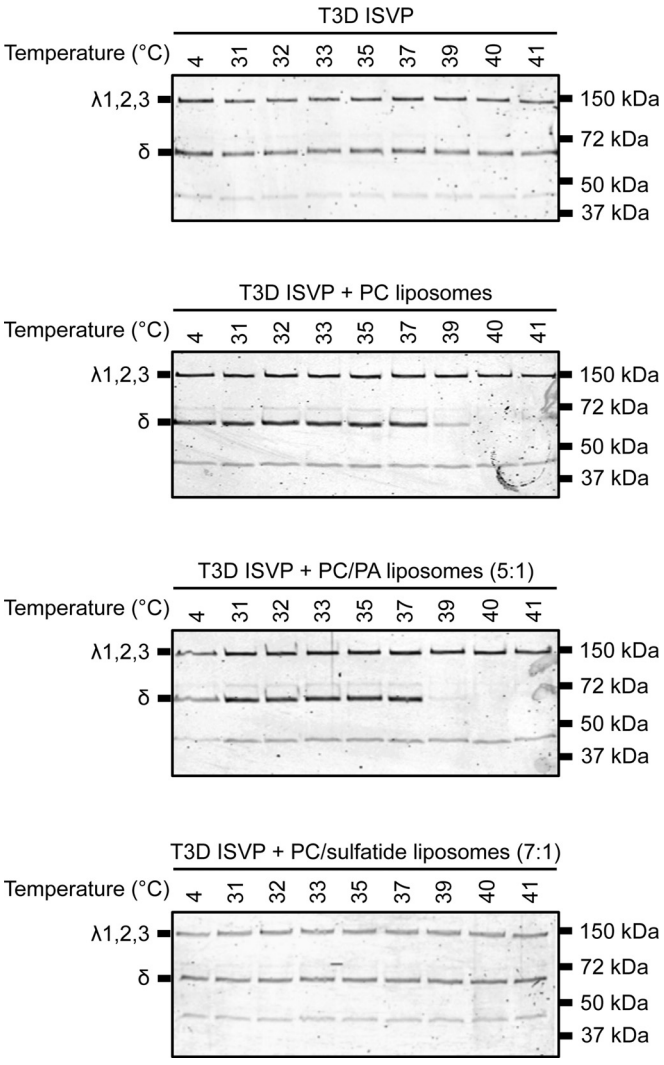

FIG 7 Liposomes composed of PC and PC-PA (5:1) promote ISVP-to-ISVP* conversion. T3D ISVPs (2×10^{12} particles/ml) were incubated in virus storage buffer supplemented with 1 mM PC, PC-PA (5:1), or PC-sulfatide (7:1) liposomes for 1 h at the indicated temperatures. After 1 h, the reaction mixtures were treated with trypsin (0.08 mg/ml) for 30 min on ice. Following digestion, the reaction mixtures were solubilized in reducing SDS sample buffer and analyzed by SDS-PAGE. The gels were Coomassie stained. The migration of the λ1,2,3 and δ bands is indicated to the left of each panel. The migration of molecular mass markers is indicated to the right of each panel.

extensively to genetically dissect various aspects of reovirus biology. During cell entry, T1L and T3D differ in the capacity to induce membrane penetration; T3D is more efficient at perforating host membranes. Using nonphysiological triggers, such as CsCl and RBCs, it has been shown that differences in cell penetration efficiency are due to the propensity to undergo ISVP-to-ISVP* conversion (42, 51, 62). To determine whether differences in membrane penetration are maintained using liposomes, we compared the capacity of T1L and T3D ISVPs to release CF from PC liposomes. Although T1L ISVPs induce CF leakage at 30°C and 42°C, the amount of CF released was significantly reduced compared to that induced by T3D ISVPs (Fig. 9). These results demonstrate that liposomes can recapitulate the differences in the cell penetration efficiency of prototype reovirus strains.

DISCUSSION

Structural rearrangements that promote cell entry of nonenveloped and enveloped viruses are predominantly triggered by low pH and/or protein-protein interactions (1–15). In this work, we provide evidence for a previously unexplored role for lipids in inducing the conformational changes required for reovirus entry. Although high concentrations of monovalent cations, such as Cs^+ and K^+, are routinely used to facilitate ISVP-to-ISVP* conversion *in vitro*, the mechanism underlying cation-induced ISVP* conversion remains undefined (42, 49, 51). In this work, we demonstrate that specific lipids, namely, PC and PE, trigger ISVP-to-ISVP* conversion, a prerequisite for membrane penetration (Fig. 6 and 7). Furthermore, we show that high concentrations of polyanions can also induce ISVP* formation (Fig. 2 and 3). Thus, our results provide the first experimental support for the idea that interactions between μ1 and lipid head groups may be involved in controlling ISVP-to-ISVP* conversion (52).

Although our results show that lipid composition plays a role in the efficiency of lipid-mediated ISVP* formation, the basis for lipid specificity is unclear. Sulfate and phosphate enhance ISVP-to-ISVP* conversion (Fig. 2 and 3). Thus, we expected lipids with anionic head groups to have a similar effect; however, our data indicate that a negative charge may not be the only factor that controls ISVP* formation. Addition of lipids with anionic head groups, such as PA or sulfatide, to PC liposomes either minimally impacted or negatively impacted the efficiency of ISVP-to-ISVP* conversion (Fig. 7). We also found that inclusion of PE, which contains a neutral, zwitterionic head group, lowers the temperature required to trigger ISVP-to-ISVP* conversion (Fig. 6). Thus, it remains unknown why certain lipid formulations promote the conformational changes required for reovirus cell entry, whereas others do not. Differences in lipid packing, which can influence membrane fluidity or rigidity, or the composition of fatty acid chains may also influence ISVP-to-ISVP* conversion. These parameters are unexplored. Furthermore, since the membrane (or liposome) composition can be varied in a potentially unlimited number of ways, we cannot rule out the possibility that the effect of certain lipids on ISVP* formation could be different in the context of different membrane compositions.

The mechanism underlying lipid-mediated ISVP* formation remains undefined. It is clear from our experiments that ISVP-to-ISVP* conversion is favored when liposomes are present (Fig. 5 to 7). As suggested by structural studies (52), we propose that ISVPs make transient interactions with lipids via their anion-binding site; these interactions promote ISVP-to-ISVP* conversion. Although liposome coflotation (or cosedimention) assays failed to reliably detect ISVP-lipid membrane interactions, we think that a reaction involving conformational rearrangements in nearly all of the 600 μ1 monomers within a single reovirus particle would not occur without at least a transient association with the membrane. The biochemical and biophysical aspects of the proposed ISVP-lipid membrane interactions are under investigation.

An obvious continuation of this work is to determine if lipids contribute to ISVP-to-ISVP* conversion within live cells. Our *in vitro* studies indicate that PC alone is sufficient to promote ISVP* formation (Fig. 6 and 7). PC constitutes a large proportion of host membranes; PC represents 40 to 50% of the phospholipid content of the plasma and endosomal mem-

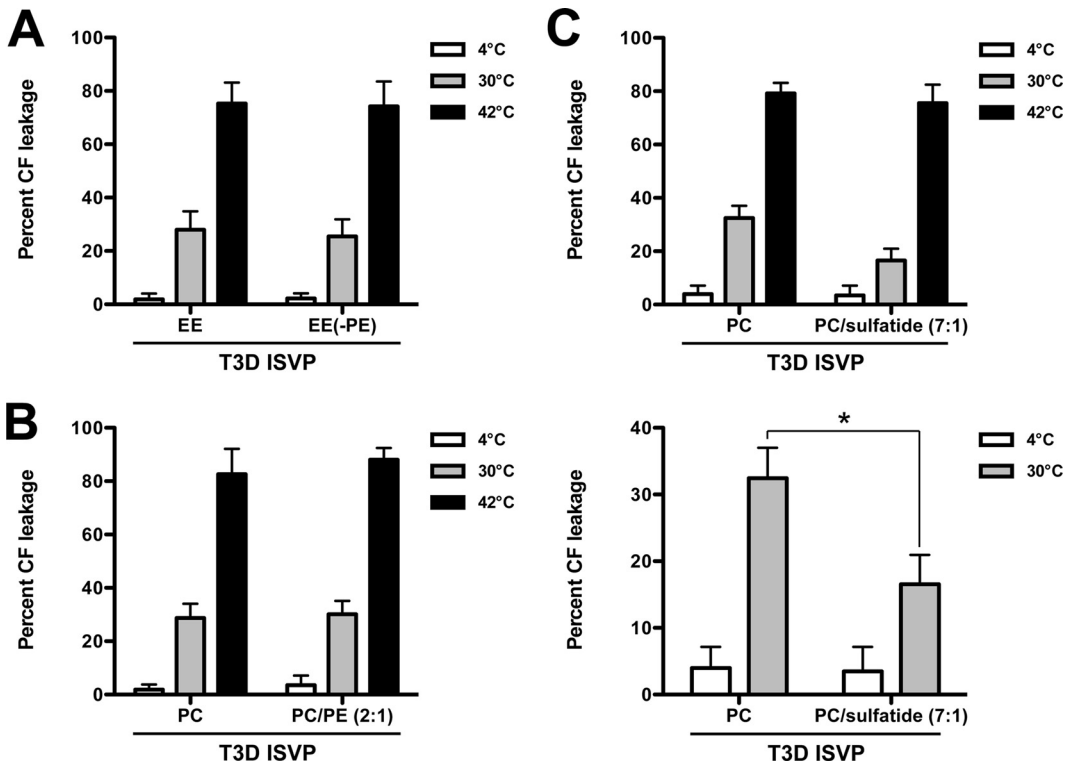

FIG 8 PC liposomes trigger ISVP-to-ISVP* conversion and pore formation more efficiently than PC-sulfatide (7:1) liposomes. T3D ISVPs (2×10^{12} particles/ml) were incubated in virus storage buffer supplemented with CF-loaded EE or EE without PE liposomes (A), CF-loaded PC or PC-PE (2:1) liposomes (B), or CF-loaded PC or PC-sulfatide (7:1) liposomes (C) for 1 h at the indicated temperatures. After 1 h, the reaction mixtures were diluted 1:50 into virus storage buffer. The samples were equilibrated at room temperature for 15 min prior to measuring fluorescence. Levels of 0 and 100% CF leakage were determined by incubating an equivalent number of CF-loaded liposomes in virus storage buffer or virus storage buffer supplemented with 0.5% Triton X-100, respectively, for 1 h at the indicated temperatures. For each condition, the mean percent CF leakage was determined from at least three independent experiments. The same data are shown in the upper and lower panels of panel C, except the range of percent CF leakage in the lower panel is reduced to highlight the differences between samples. Error bars indicate standard deviations. *P* values were calculated using Student's *t* test. *, $P \leq 0.05$.

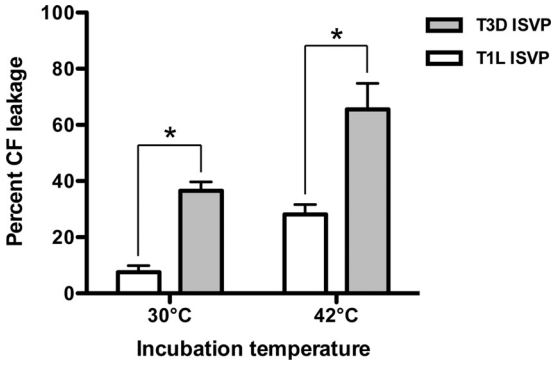

FIG 9 T3D ISVPs induce pore formation in PC liposomes more efficiently than T1L ISVPs. T3D or T1L ISVPs (2×10^{12} particles/ml) were incubated in virus storage buffer supplemented with CF-loaded PC liposomes for 1 h at the indicated temperatures. After 1 h, the reaction mixtures were diluted 1:50 into virus storage buffer. The samples were equilibrated at room temperature for 15 min prior to measuring fluorescence. Levels of 0 and 100% CF leakage were determined by incubating an equivalent number of CF-loaded liposomes in virus storage buffer or virus storage buffer supplemented with 0.5% Triton X-100, respectively, for 1 h at the indicated temperatures. For each condition, the mean percent CF leakage was determined from at least three independent experiments. Error bars indicate standard deviations. *P* values were calculated using Student's *t* test. *, $P \leq 0.05$.

branes (60), two sites where ISVPs are known to penetrate host cells (34–37, 40, 41, 48). Consequently, when we attempted to enzymatically deplete PC with phospholipases, we observed a loss in cell viability, which precluded us from assessing the impact of PC on ISVP-to-ISVP* conversion within infected cells (data not shown).

Reovirus strain T3D perforates host membranes more efficiently than T1L; the μ1 protein governs this property (62). Multiple *in vitro* studies using nonphysiological triggers, such as CsCl and RBCs, revealed that the difference in membrane penetration efficiency is related to the capacity of T3D and T1L to undergo ISVP-to-ISVP* conversion (42, 51). In this study, we demonstrate that the differences in the membrane penetration efficiency of T3D and T1L can be recapitulated using a trigger that is likely encountered by the virus within an infected cell (Fig. 8). Structural studies of the T1L μ1 homotrimer revealed an anion-binding site within the μ1 δ region (Fig. 1B) (52). It was proposed that main-chain amide groups within this loop interact with lipids. The μ1 proteins of T3D and T1L differ by only 15 amino acids (51). Interestingly, 2 of the 15 polymorphisms are found in the protein sequence that corresponds to the proposed anion-binding site (Fig. 1D). Although our studies do not address which portion of μ1 interacts with lipids, it is possible that polymorphisms within the anion-binding site influence the capacity to undergo lipid-mediated ISVP-to-ISVP* conversion.

Host membranes represent a physical barrier that prevents virus invasion. To overcome this barrier, nonenveloped and enveloped viruses sense one or more cellular cues that trigger conformational changes within viral proteins. Viruses can interact with host proteins, such as receptors, which facilitates cell penetration at the plasma or endosomal membrane (6–11). Alternatively, some viruses respond to the low-pH environment of the endosome (1–5). These strategies ensure that viruses undergo structural rearrangements only in an environment that preserves viral infectivity and allows establishment of a productive infection. Reoviruses are different in this regard, as they can enter either at the plasma membrane or from within the host endosome. In the intestines, ISVPs penetrate cells directly at the plasma membrane (34–37). In most other cell types, the virus is endocytosed (23–28) and ISVPs perforate the endosomal membrane (40, 41, 48). Instead of depending on two distinct host factors to mediate entry, our work reveals that reoviruses evolved a strategy to sense lipids, a host factor that is common to the plasma and endosomal membranes. Thus, a unique triggering mechanism that relies on virus-lipid interactions demonstrates that host membranes are not merely passive barriers that must be overcome. Instead, this work shows that host lipids can play an active role in mediating virus entry.

ACKNOWLEDGMENTS

We thank Karl Boehme, Tuli Mukhopadhyay, and Kevin Sokoloski for helpful suggestions and reviews of the manuscript.

FUNDING INFORMATION

HHS | NIH | National Institute of Allergy and Infectious Diseases (NIAID) provided funding to Pranav Danthi under grant number 1R01AI110637.

The funders had no role in study design, data collection and interpretation, or the decision to submit the work for publication.

REFERENCES

1. **Bayer N, Schober D, Huttinger M, Blaas D, Fuchs R.** 2001. Inhibition of clathrin-dependent endocytosis has multiple effects on human rhinovirus serotype 2 cell entry. J Biol Chem **276:**3952–3962. http://dx.doi.org/10.1074/jbc.M004722200.
2. **Bayer N, Schober D, Prchla E, Murphy RF, Blaas D, Fuchs R.** 1998. Effect of bafilomycin A1 and nocodazole on endocytic transport in HeLa cells: implications for viral uncoating and infection. J Virol **72:**9645–9655.
3. **Stegmann T, Booy FP, Wilschut J.** 1987. Effects of low pH on influenza virus. Activation and inactivation of the membrane fusion capacity of the hemagglutinin. J Biol Chem **262:**17744–17749.
4. **White J, Helenius A, Gething MJ.** 1982. Haemagglutinin of influenza virus expressed from a cloned gene promotes membrane fusion. Nature **300:**658–659. http://dx.doi.org/10.1038/300658a0.
5. **Yoshimura A, Ohnishi S.** 1984. Uncoating of influenza virus in endosomes. J Virol **51:**497–504.
6. **Kaplan G, Freistadt MS, Racaniello VR.** 1990. Neutralization of poliovirus by cell receptors expressed in insect cells. J Virol **64:**4697–4702.
7. **Perez L, Carrasco L.** 1993. Entry of poliovirus into cells does not require a low-pH step. J Virol **67:**4543–4548.
8. **Fricks CE, Hogle JM.** 1990. Cell-induced conformational change in poliovirus: externalization of the amino terminus of VP1 is responsible for liposome binding. J Virol **64:**1934–1945.
9. **Fuller AO, Lee WC.** 1992. Herpes simplex virus type 1 entry through a cascade of virus-cell interactions requires different roles of gD and gH in penetration. J Virol **66:**5002–5012.
10. **Fuller AO, Santos RE, Spear PG.** 1989. Neutralizing antibodies specific for glycoprotein H of herpes simplex virus permit viral attachment to cells but prevent penetration. J Virol **63:**3435–3443.
11. **Wittels M, Spear PG.** 1991. Penetration of cells by herpes simplex virus does not require a low pH-dependent endocytic pathway. Virus Res **18:**271–290. http://dx.doi.org/10.1016/0168-1702(91)90024-P.
12. **Mothes W, Boerger AL, Narayan S, Cunningham JM, Young JA.** 2000. Retroviral entry mediated by receptor priming and low pH triggering of an envelope glycoprotein. Cell **103:**679–689. http://dx.doi.org/10.1016/S0092-8674(00)00170-7.
13. **Inoue T, Tsai B.** 2011. A large and intact viral particle penetrates the endoplasmic reticulum membrane to reach the cytosol. PLoS Pathog **7:**e1002037. http://dx.doi.org/10.1371/journal.ppat.1002037.
14. **Magnuson B, Rainey EK, Benjamin T, Baryshev M, Mkrtchian S, Tsai B.** 2005. ERp29 triggers a conformational change in polyomavirus to stimulate membrane binding. Mol Cell **20:**289–300. http://dx.doi.org/10.1016/j.molcel.2005.08.034.
15. **Rainey-Barger EK, Magnuson B, Tsai B.** 2007. A chaperone-activated nonenveloped virus perforates the physiologically relevant endoplasmic reticulum membrane. J Virol **81:**12996–13004. http://dx.doi.org/10.1128/JVI.01037-07.
16. **Dryden KA, Wang G, Yeager M, Nibert ML, Coombs KM, Furlong DB, Fields BN, Baker TS.** 1993. Early steps in reovirus infection are associated with dramatic changes in supramolecular structure and protein conformation: analysis of virions and subviral particles by cryoelectron microscopy and image reconstruction. J Cell Biol **122:**1023–1041. http://dx.doi.org/10.1083/jcb.122.5.1023.
17. **Knipe DM, Howley PM (ed).** 2013. Fields virology, 6th ed. Lippincott Williams & Wilkins, Philadelphia, PA.
18. **Barton ES, Connolly JL, Forrest JC, Chappell JD, Dermody TS.** 2001. Utilization of sialic acid as a coreceptor enhances reovirus attachment by multistep adhesion strengthening. J Biol Chem **276:**2200–2211. http://dx.doi.org/10.1074/jbc.M004680200.
19. **Chappell JD, Duong JL, Wright BW, Dermody TS.** 2000. Identification of carbohydrate-binding domains in the attachment proteins of type 1 and type 3 reoviruses. J Virol **74:**8472–8479. http://dx.doi.org/10.1128/JVI.74.18.8472-8479.2000.
20. **Gentsch JR, Pacitti AF.** 1987. Differential interaction of reovirus type 3 with sialylated receptor components on animal cells. Virology **161:**245–248. http://dx.doi.org/10.1016/0042-6822(87)90192-9.
21. **Gentsch JR, Pacitti AF.** 1985. Effect of neuraminidase treatment of cells and effect of soluble glycoproteins on type 3 reovirus attachment to murine L cells. J Virol **56:**356–364.
22. **Paul RW, Choi AH, Lee PW.** 1989. The alpha-anomeric form of sialic acid is the minimal receptor determinant recognized by reovirus. Virology **172:**382–385. http://dx.doi.org/10.1016/0042-6822(89)90146-3.
23. **Borsa J, Morash BD, Sargent MD, Copps TP, Lievaart PA, Szekely JG.** 1979. Two modes of entry of reovirus particles into L cells. J Gen Virol **45:**161–170. http://dx.doi.org/10.1099/0022-1317-45-1-161.
24. **Borsa J, Sargent MD, Lievaart PA, Copps TP.** 1981. Reovirus: evidence for a second step in the intracellular uncoating and transcriptase activation process. Virology **111:**191–200. http://dx.doi.org/10.1016/0042-6822(81)90664-4.
25. **Ehrlich M, Boll W, Van Oijen A, Hariharan R, Chandran K, Nibert ML, Kirchhausen T.** 2004. Endocytosis by random initiation and stabilization of clathrin-coated pits. Cell **118:**591–605. http://dx.doi.org/10.1016/j.cell.2004.08.017.
26. **Maginnis MS, Forrest JC, Kopecky-Bromberg SA, Dickeson SK, Santoro SA, Zutter MM, Nemerow GR, Bergelson JM, Dermody TS.** 2006. Beta1 integrin mediates internalization of mammalian reovirus. J Virol **80:**2760–2770. http://dx.doi.org/10.1128/JVI.80.6.2760-2770.2006.
27. **Maginnis MS, Mainou BA, Derdowski A, Johnson EM, Zent R, Dermody TS.** 2008. NPXY motifs in the beta1 integrin cytoplasmic tail are required for functional reovirus entry. J Virol **82:**3181–3191. http://dx.doi.org/10.1128/JVI.01612-07.
28. **Sturzenbecker LJ, Nibert M, Furlong D, Fields BN.** 1987. Intracellular digestion of reovirus particles requires a low pH and is an essential step in the viral infectious cycle. J Virol **61:**2351–2361.
29. **Baer GS, Dermody TS.** 1997. Mutations in reovirus outer-capsid protein sigma3 selected during persistent infections of L cells confer resistance to protease inhibitor E64. J Virol **71:**4921–4928.
30. **Chang CT, Zweerink HJ.** 1971. Fate of parental reovirus in infected cell. Virology **46:**544–555. http://dx.doi.org/10.1016/0042-6822(71)90058-4.
31. **Dermody TS, Nibert ML, Wetzel JD, Tong X, Fields BN.** 1993. Cells and viruses with mutations affecting viral entry are selected during persistent infections of L cells with mammalian reoviruses. J Virol **67:**2055–2063.
32. **Ebert DH, Deussing J, Peters C, Dermody TS.** 2002. Cathepsin L and

cathepsin B mediate reovirus disassembly in murine fibroblast cells. J Biol Chem **277:**24609–24617. http://dx.doi.org/10.1074/jbc.M201107200.
33. **Silverstein SC, Astell C, Levin DH, Schonberg M, Acs G.** 1972. The mechanisms of reovirus uncoating and gene activation in vivo. Virology **47:**797–806. http://dx.doi.org/10.1016/0042-6822(72)90571-5.
34. **Amerongen HM, Wilson GA, Fields BN, Neutra MR.** 1994. Proteolytic processing of reovirus is required for adherence to intestinal M cells. J Virol **68:**8428–8432.
35. **Bass DM, Bodkin D, Dambrauskas R, Trier JS, Fields BN, Wolf JL.** 1990. Intraluminal proteolytic activation plays an important role in replication of type 1 reovirus in the intestines of neonatal mice. J Virol **64:**1830–1833.
36. **Bodkin DK, Nibert ML, Fields BN.** 1989. Proteolytic digestion of reovirus in the intestinal lumens of neonatal mice. J Virol **63:**4676–4681.
37. **Nygaard RM, Golden JW, Schiff LA.** 2012. Impact of host proteases on reovirus infection in the respiratory tract. J Virol **86:**1238–1243. http://dx.doi.org/10.1128/JVI.06429-11.
38. **Borsa J, Copps TP, Sargent MD, Long DG, Chapman JD.** 1973. New intermediate subviral particles in the in vitro uncoating of reovirus virions by chymotrypsin. J Virol **11:**552–564.
39. **Joklik WK.** 1972. Studies on the effect of chymotrypsin on reovirions. Virology **49:**700–715. http://dx.doi.org/10.1016/0042-6822(72)90527-2.
40. **Agosto MA, Ivanovic T, Nibert ML.** 2006. Mammalian reovirus, a nonfusogenic nonenveloped virus, forms size-selective pores in a model membrane. Proc Natl Acad Sci U S A **103:**16496–16501. http://dx.doi.org/10.1073/pnas.0605835103.
41. **Ivanovic T, Agosto MA, Zhang L, Chandran K, Harrison SC, Nibert ML.** 2008. Peptides released from reovirus outer capsid form membrane pores that recruit virus particles. EMBO J **27:**1289–1298. http://dx.doi.org/10.1038/emboj.2008.60.
42. **Chandran K, Farsetta DL, Nibert ML.** 2002. Strategy for nonenveloped virus entry: a hydrophobic conformer of the reovirus membrane penetration protein micro 1 mediates membrane disruption. J Virol **76:**9920–9933. http://dx.doi.org/10.1128/JVI.76.19.9920-9933.2002.
43. **Borsa J, Long DG, Sargent MD, Copps TP, Chapman JD.** 1974. Reovirus transcriptase activation in vitro: involvement of an endogenous uncoating activity in the second stage of the process. Intervirology **4:**171–188.
44. **Nibert ML, Schiff LA, Fields BN.** 1991. Mammalian reoviruses contain a myristoylated structural protein. J Virol **65:**1960–1967.
45. **Nibert ML, Odegard AL, Agosto MA, Chandran K, Schiff LA.** 2005. Putative autocleavage of reovirus mu1 protein in concert with outer-capsid disassembly and activation for membrane permeabilization. J Mol Biol **345:**461–474. http://dx.doi.org/10.1016/j.jmb.2004.10.026.
46. **Zhang X, Ji Y, Zhang L, Harrison SC, Marinescu DC, Nibert ML, Baker TS.** 2005. Features of reovirus outer capsid protein mu1 revealed by electron cryomicroscopy and image reconstruction of the virion at 7.0 angstrom resolution. Structure **13:**1545–1557. http://dx.doi.org/10.1016/j.str.2005.07.012.
47. **Odegard AL, Chandran K, Zhang X, Parker JS, Baker TS, Nibert ML.** 2004. Putative autocleavage of outer capsid protein micro1, allowing release of myristoylated peptide micro1N during particle uncoating, is critical for cell entry by reovirus. J Virol **78:**8732–8745. http://dx.doi.org/10.1128/JVI.78.16.8732-8745.2004.
48. **Zhang L, Agosto MA, Ivanovic T, King DS, Nibert ML, Harrison SC.** 2009. Requirements for the formation of membrane pores by the reovirus myristoylated micro1N peptide. J Virol **83:**7004–7014. http://dx.doi.org/10.1128/JVI.00377-09.
49. **Borsa J, Sargent MD, Long DG, Chapman JD.** 1973. Extraordinary effects of specific monovalent cations on activation of reovirus transcriptase by chymotrypsin in vitro. J Virol **11:**207–217.
50. **Middleton JK, Severson TF, Chandran K, Gillian AL, Yin J, Nibert ML.** 2002. Thermostability of reovirus disassembly intermediates (ISVPs) correlates with genetic, biochemical, and thermodynamic properties of major surface protein mu1. J Virol **76:**1051–1061. http://dx.doi.org/10.1128/JVI.76.3.1051-1061.2002.
51. **Sarkar P, Danthi P.** 2010. Determinants of strain-specific differences in efficiency of reovirus entry. J Virol **84:**12723–12732. http://dx.doi.org/10.1128/JVI.01385-10.
52. **Liemann S, Chandran K, Baker TS, Nibert ML, Harrison SC.** 2002. Structure of the reovirus membrane-penetration protein, mu1, in a complex with is protector protein, sigma3. Cell **108:**283–295. http://dx.doi.org/10.1016/S0092-8674(02)00612-8.
53. **Bossemeyer D.** 1994. The glycine-rich sequence of protein kinases: a multifunctional element. Trends Biochem Sci **19:**201–205. http://dx.doi.org/10.1016/0968-0004(94)90022-1.
54. **Saraste M, Sibbald PR, Wittinghofer A.** 1990. The P-loop—a common motif in ATP- and GTP-binding proteins. Trends Biochem Sci **15:**430–434. http://dx.doi.org/10.1016/0968-0004(90)90281-F.
55. **Kobayashi T, Ooms LS, Ikizler M, Chappell JD, Dermody TS.** 2010. An improved reverse genetics system for mammalian orthoreoviruses. Virology **398:**194–200. http://dx.doi.org/10.1016/j.virol.2009.11.037.
56. **Kobayashi T, Antar AA, Boehme KW, Danthi P, Eby EA, Guglielmi KM, Holm GH, Johnson EM, Maginnis MS, Naik S, Skelton WB, Wetzel JD, Wilson GJ, Chappell JD, Dermody TS.** 2007. A plasmid-based reverse genetics system for animal double-stranded RNA viruses. Cell Host Microbe **1:**147–157. http://dx.doi.org/10.1016/j.chom.2007.03.003.
57. **Furlong DB, Nibert ML, Fields BN.** 1988. Sigma 1 protein of mammalian reoviruses extends from the surfaces of viral particles. J Virol **62:**246–256.
58. **Mendez II, Hermann LL, Hazelton PR, Coombs KM.** 2000. A comparative analysis of Freon substitutes in the purification of reovirus and calicivirus. J Virol Methods **90:**59–67. http://dx.doi.org/10.1016/S0166-0934(00)00217-2.
59. **Smith RE, Zweerink HJ, Joklik WK.** 1969. Polypeptide components of virions, top component and cores of reovirus type 3. Virology **39:**791–810. http://dx.doi.org/10.1016/0042-6822(69)90017-8.
60. **Kobayashi T, Stang E, Fang KS, de Moerloose P, Parton RG, Gruenberg J.** 1998. A lipid associated with the antiphospholipid syndrome regulates endosome structure and function. Nature **392:**193–197. http://dx.doi.org/10.1038/32440.
61. **Kushi Y, Arita M, Ishizuka I, Kasama T, Fredman P, Handa S.** 1996. Sulfatide is expressed in both erythrocytes and platelets of bovine origin. Biochim Biophys Acta **1304:**254–262. http://dx.doi.org/10.1016/S0005-2760(96)00125-7.
62. **Lucia-Jandris P, Hooper JW, Fields BN.** 1993. Reovirus M2 gene is associated with chromium release from mouse L cells. J Virol **67:**5339–5345.